Small changes in enzyme function can lead to surprisingly large fitness effects during adaptive evolution of antibiotic resistance

Katarzyna Walkiewicz[a,1], Andres S. Benitez Cardenas[a,1], Christine Sun[a], Colin Bacorn[a], Gerda Saxer[a], and Yousif Shamoo[a,b,2]

Departments of [a]Biochemistry and Cell Biology and [b]Ecology and Evolutionary Biology, Rice University, Houston, TX 77005-1892

Edited by Richard E. Lenski, Michigan State University, East Lansing, MI, and approved November 12, 2012 (received for review June 7, 2012)

In principle, evolutionary outcomes could be largely predicted if all of the relevant physicochemical variants of a particular protein function under selection were known and integrated into an appropriate physiological model. We have tested this principle by generating a family of variants of the tetracycline resistance protein TetX2 and identified the physicochemical properties most correlated with organismal fitness. Surprisingly, small changes in the $K_{m(MCN)}$, less than twofold, were sufficient to produce highly successful adaptive mutants over clinically relevant drug concentrations. We then built a quantitative model directly relating the in vitro physicochemical properties of the mutant enzymes to the growth rates of bacteria carrying a single chromosomal copy of the *tet(X2)* variants over a wide range of minocycline (MCN) concentrations. Importantly, this model allows the prediction of enzymatic properties directly from cellular growth rates as well as the physicochemical-fitness landscape of TetX2. Using experimental evolution and deep sequencing to monitor the allelic frequencies of the seven most biochemically efficient TetX2 mutants in 10 independently evolving populations, we showed that the model correctly predicted the success of the two most beneficial variants $tet(X2)_{T280A}$ and $tet(X2)_{N371I}$. The structure of the most efficient variant, $TetX2_{T280A}$, in complex with MCN at 2.7 Å resolution suggests an indirect effect on enzyme kinetics. Taken together, these findings support an important role for readily accessible small steps in protein evolution that can, in turn, greatly increase the fitness of an organism during natural selection.

experimental evolution | genome to phenome | oxidoreductase

What determines success or failure of variants within a population undergoing selection? To answer this challenging question, experimental evolution, genomics, and biochemistry have proved to be powerful approaches to the formulation of specific and testable hypotheses that can be validated in a quantitative manner. Most recently, experimental evolution has provided a wealth of insights into epistasis (1–3), adaptive convergence among populations (4, 5), and the role of mutation supply (6, 7) in asexual populations (8). Dean and Thornton coined the term "functional synthesis" to encompass the increasingly relevant role for molecular biology, biochemistry, and biophysics in elucidating a strong quantitative link between changes in genomes (genotype) to their resultant changes in molecular properties (phenotype) and fitness, the property that selection acts upon (9). Dykhuizen and coworkers were among the first to recognize the importance of the functional synthesis when they successfully modeled the adaptive landscape of the lactose operon to quantitatively predict growth rates (10). Whereas the qualitative link between an enzyme function under selection and fitness is typically straightforward, it has proved very challenging to predict how specific adaptive changes in readily measurable in vitro biophysical properties of a protein can be used to make accurate predictions of growth rates and evolutionary outcomes over a range of selective conditions. In addition to physicochemical properties, interactions among different mutants in a population such as clonal interference, the stochasticity with which new mutations arise, and the fact that even beneficial mutations can be lost through drift when they are very rare affect evolutionary dynamics (11).

We tested two important principles that are the key to the hypothesis that a careful physicochemical analysis of potential adaptive mutants can be used to predict evolutionary dynamics within large asexual populations undergoing selection (Fig. 1): first, that the physicochemical analysis of potential adaptive mutants and the development of an appropriate physiological model can quantitatively predict growth rates of bacteria carrying these alleles over a broad range of selective conditions; and second, that these ex vivo predictions for growth would predict the evolutionary dynamics in a population undergoing selection.

To test these principles, we used in vitro error-prone mutagenesis to identify adaptive mutants of *Bacteroides thetaiotaomicron* TetX2 that conferred similar or increased resistance to minocycline (MCN) within 1-nt change of the original sequence. From the TetX2 library, seven potential adaptive mutants were identified and characterized biochemically to determine their steady-state enzyme kinetics. Each adaptive *tet(X2)* allele was then introduced as a single chromosomal copy into the *Escherichia coli spc* operon that encodes 10 ribosomal proteins, and their growth rates were measured over a wide range of MCN concentrations. Using data from a combination of the in vitro kinetics and in vivo expression level measurements we were able to build a mathematical model that accurately and quantitatively predicted the bacterial growth rates from biochemical first principles such as k_{cat}, $K_{m(MCN)}$, and $K_{m(NADPH)}$ and steady-state expression levels. An unexpected finding from these studies was the critical role of very small changes in physicochemical parameters and their outsized effects on bacterial growth rates over the relevant MCN selection range. For example, less than a twofold change in K_m and <20% change in k_{cat} toward MCN for the best adaptive mutant [$tet(X2)_{T280A}$] increased growth rate 240% at 10 μg/mL MCN. After establishing the relationship of biochemical parameters to growth kinetics of the seven most successful adaptive TetX2 mutants, experimental evolution was used to monitor adaptation in 10 bacterial populations undergoing selection to increasing amounts of MCN.

The broad success of the model in building a quantitative link between enzyme function and growth rates suggests that, under specific conditions, growth rates over a wide range of selective conditions can provide a robust and high-throughput means of estimating kinetic parameters for libraries of enzyme variants

Author contributions: Y.S. designed research; K.W., A.S.B.C., C.S., C.B., and G.S. performed research; K.W., A.S.B.C., C.S., C.B., G.S., and Y.S. analyzed data; and K.W., A.S.B.C., G.S., and Y.S. wrote the paper.

The authors declare no conflict of interest.

This article is a PNAS Direct Submission.

Data deposition: The atomic coordinates and structure factors have been deposited in the Protein Data Bank, www.pdb.org (PDB ID code 3V3N).

[1]K.W. and A.S.B.C. contributed equally to this work.

[2]To whom correspondence should be addressed. E-mail: shamoo@rice.edu.

This article contains supporting information online at www.pnas.org/lookup/suppl/doi:10.1073/pnas.1209335110/-/DCSupplemental.

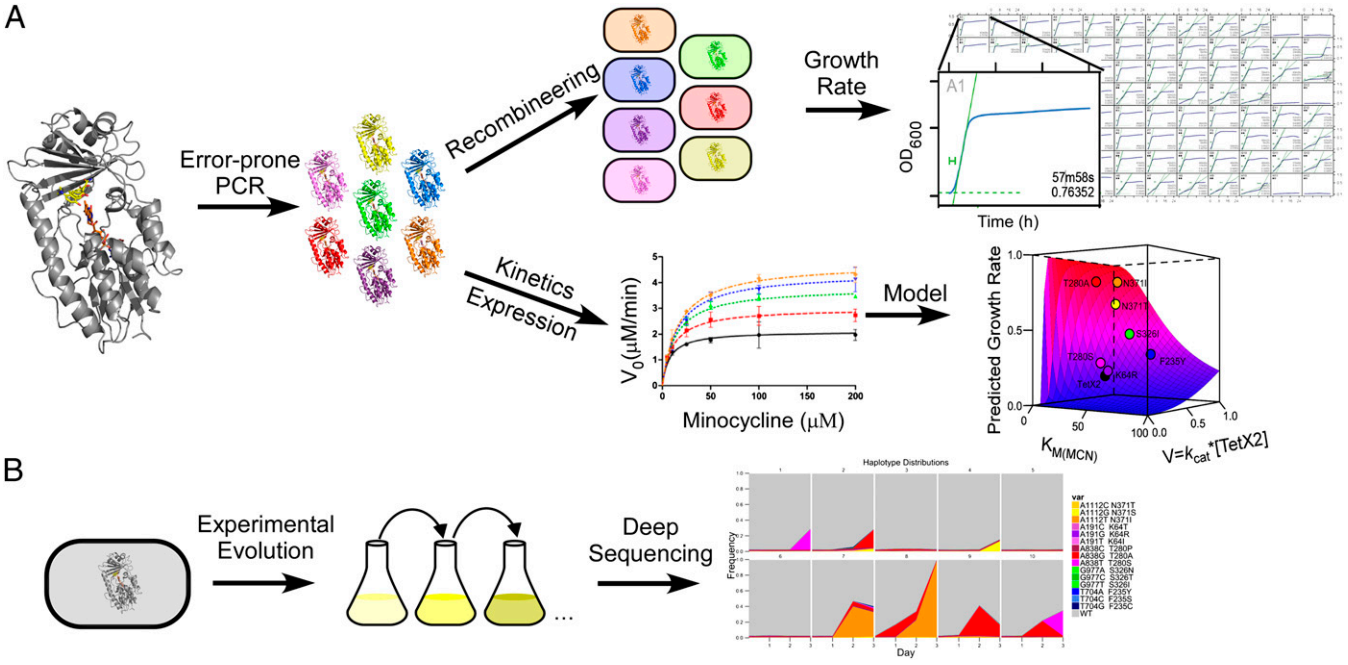

Fig. 1. Predicting evolutionary outcomes using experimental evolution and biochemistry. (*A*) Changes in physicochemical properties of adaptive mutants that correlate with changes in fitness (growth rates) are determined and used to model the in vivo performance of the organisms expressing mutant alleles. (*B*) The predictions based on the mathematical model are tested by monitoring allelic frequencies, using deep sequencing.

without arduous purification of the individual protein variants. This approach can further expand our understanding of protein evolution and the physicochemical principles underlying natural selection. Most importantly, these findings highlight the critical relationship of small changes in enzyme performance to highly relevant changes in organismal fitness during natural selection.

Results

TetX2 Variants Expressed from the Chromosomal *spc* Operon of *E. coli* Directly Drive Fitness to Minocycline. The success of cells with newly acquired mutations in an evolving population depends strongly on the fitness benefit conferred by the mutations under specific conditions of selection. Elucidating a physicochemical basis for evolutionary dynamics is made easier if relevant adaptive mutations have been identified and characterized. In vitro error-prone mutagenesis was used to identify potential single-point mutations of *tet(X2)* that could be candidates for natural selection in a bacterial population undergoing adaptation to increasing MCN concentrations (Fig. S1). Seven adaptive mutants that conferred equal or greater minimal inhibitory concentrations (MICs) to MCN than wild type *tet(X2)* were identified from the library (Table 1).

As MCN concentrations are increased, the ability of a particular *tet(X2)* variant to reduce cytoplasmic MCN concentrations to a point sufficient to maintain wild-type growth rates becomes increasingly difficult until TetX2 is unable to maintain a sufficiently low steady-state concentration of MCN, resulting in slower growth rates. Here, we use absolute growth rate as a measure for fitness because it provides a more accurate link between physicochemical properties of TetX2 and bacterial growth than MICs. We introduced each of the adaptive *tet(X2)* alleles as a single chromosomal copy into the *spc* operon of *E. coli* BW25113 by Red short-homology recombineering (12) and measured the growth rates of *E. coli* BW25113 and the eight recombineered strains over a range of MCN concentrations that correspond to Food and Drug Administration guidelines for the susceptibility testing of *Enterobacteria* at 37 °C (13) (Fig. S2 and Table S1).

The growth rates of the wild-type *tet(X2)* and all of the *tet(X2)* mutants were significantly lower than the growth rates of the host BW25113 without *tet(X2)*, indicating a fitness cost of 4.6% to carrying a *tet(X2)* allele (planned comparison between host without and strains with *tet(X2)* alleles: $F_{1,23} = 25.9$, $P < 0.0001$). As expected, with increasing MCN concentration, the growth rates of all *tet(X2)* mutants decreased (Fig. 2). Three mutants, $tet(X2)_{F235Y}$, $tet(X2)_{S326I}$, and $tet(X2)_{N371T}$, exhibited intermediate fitness compared with the most successful mutant, $tet(X2)_{T280A}$. At 32 μM MCN, the breakpoint for clinical resistance, $tet(X2)_{T280A}$ was 1.7, 1.6, and 1.2 times fitter than $tet(X2)_{F235Y}$, $tet(X2)_{S326I}$, and $tet(X2)_{N371T}$, respectively. $Tet(X2)_{N371I}$ and $tet(X2)_{T280A}$ had the

Table 1. Steady-state kinetic parameters for wild-type TetX2 and adaptive mutants

	$K_{m(MCN)}$, μM	$K_{m(NADPH)}$, μM	k_{cat} ($V_{max}/[E_{total}]$), s^{-1}	$k_{cat}/K_{m(MCN)}$, $\mu M^{-1}\cdot s^{-1}$	$k_{cat}/K_{m(NADPH)}$, $\mu M^{-1}\cdot s^{-1}$	Δ growth rates at 32 μM MCN, %*
WT	35 ± 1.9	75 ± 4.1	0.34 ± 0.01	0.010 ± 0.0006	0.004 ± 0.0003	100
T280A	18 ± 0.9	18 ± 1.1	0.43 ± 0.01	0.024 ± 0.0013	0.024 ± 0.0016	540
N371I	18 ± 1.9	64 ± 6.3	0.37 ± 0.02	0.020 ± 0.0024	0.006 ± 0.0006	530
N371T	24 ± 2.1	130 ± 11	0.40 ± 0.02	0.017 ± 0.0017	0.003 ± 0.0003	440
S326I	37 ± 2.8	73 ± 5.5	0.36 ± 0.01	0.010 ± 0.0008	0.005 ± 0.0004	340
F235Y	54 ± 6.1	99 ± 11	0.32 ± 0.06	0.006 ± 0.0013	0.003 ± 0.0007	320
K64R	36 ± 4.6	110 ± 15	0.32 ± 0.03	0.009 ± 0.0014	0.003 ± 0.0005	86
T280S	30 ± 3.4	100 ± 14	0.18 ± 0.01	0.006 ± 0.0008	0.002 ± 0.0003	65

*Changes in growth rates of mutant alleles are relative to the wild-type *tet(X2)* growth rate set at 100%.

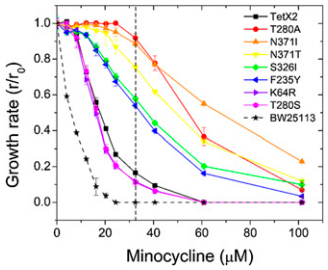

Fig. 2. Similar growth rate profiles for *tet(X2)*$_{T280A}$ and *tet(X2)*$_{N371I}$ suggest that both mutants should have equal opportunity for success during selection. Shown are growth rates of the ancestral *E. coli* BW25113 strains expressing a chromosomal copy of *tet(X2)*$_{wild\ type}$ and seven variants. The clinical breakpoint for resistance (dashed line) to MCN is 16 μg/mL (32 μM). At lower MCN concentrations (2 and 4 μg/mL), growth rates (e.g., fitness) for all of the variants are comparable. At higher MCN concentrations, *tet(X2)*$_{T280A}$ and *tet(X2)*$_{N371I}$ exhibit the fastest growth rates, whereas the growth rates of *tet(X2)*$_{T280S}$ and *tet(X2)*$_{K64R}$ are significantly lower and resemble the growth of wild-type *tet(X2)*. Error bars correspond to the SD among measurements for independent growth assays for three individual colonies.

fastest growth rates at intermediate and high MCN concentrations, suggesting that both mutants would have comparable success in a population during selection at MCN concentrations that would be used clinically (13).

Adaptive Mutations to TetX2 That Determine Evolutionary Dynamics over a Clinically Relevant MCN Range Show Remarkably Small Changes in Kinetic Performance. The in vivo resistance of bacteria expressing each candidate *tet(X2)* mutant was directly linked to the in vitro catalytic properties of TetX2 through steady-state activity assays that measure the kinetics of MCN inactivation in vitro. The catalytic profiles exhibited by TetX2 adaptive mutants suggest that surprisingly small changes in TetX2 steady-state kinetic parameters have large consequences on the in vivo performance of the organisms in a population. TetX2 is a flavin-dependent monooxygenase that regioselectively hydroxylates tetracyclines in a reaction that requires both NADPH and molecular oxygen (14). The initial velocities of MCN inactivation were measured at various NADPH and MCN concentrations (Table 1), and the steady-state kinetic parameters [$K_{m(MCN)}$, $K_{m(NADPH)}$, and k_{cat}] for each purified mutant enzyme were determined. Overall, the adaptive mutants exhibited similar mechanistic behaviors. As shown in Fig. 3*A*, the initial velocities of the enzyme (here, TetX2$_{T280A}$) at different MCN concentrations increased with increasing NADPH, which, in turn, resulted in an increase in $V_{max(obs)}$. In addition, the $K_{m(obs)}$ also increases with increasing NADPH concentrations, which suggests that only binary complexes of the enzyme with these substrates can occur and that MCN and NADPH cannot be bound simultaneously in the active site (i.e., no ternary TetX2:MCN:NADPH complex forms). Lineweaver–Burke plots of initial velocities vs. MCN concentration strongly support a ping-pong mechanism for TetX2 inactivation of MCN (Fig. 3*B*). Therefore, the kinetic parameters $K_{m(MCN)}$, $K_{m(NADPH)}$, and k_{cat} ($V_{max} = k_{cat} \times [E]$, where E is total enzyme concentration) reported in Table 1 were calculated by fitting initial velocities to a simple, rapid equilibrium ping-pong model for the two substrates MCN and NADPH (Eq. **S1** and Schemes S1 and S2) (15).

Surprisingly, the changes in K_ms toward MCN and NADPH, as well as k_{cat}, that determined the growth rates within the individual strains and their subsequent success or failure during experimental evolution within populations are remarkably small (Table 1). The most successful TetX2 mutant, TetX2$_{T280A}$, had less than a twofold decrease in K_m (18 μM) for MCN and a fourfold decrease for NADPH (18 μM) compared with the wild-type enzyme [$K_{m(MCN)}$ = 35 μM, $K_{m(NADPH)}$ = 75 μM]. All seven TetX2 mutants isolated from in vitro mutagenesis had a measured k_{cat} comparable to that of wild-type TetX2 (k_{cat} = 0.34 s^{-1}) and although TetX$_{T280A}$ had the highest k_{cat} (0.43 s^{-1}), the increase was quite modest (~20%). The efficiencies of the two catalytic steps, first, FAD reduction by NADPH and, second, hydroxylation of MCN, were altered by at most fivefold (TetX2$_{T280A}$). TetX2$_{K64R}$ had no significant change in the $K_{m(MCN)}$ but a higher $K_{m(NADPH)}$ and no change in k_{cat}, which is largely consistent with its in vivo growth rates.

The subtle changes in kinetic parameters of the most successful mutants TetX2$_{T280A}$ and TetX2$_{N371I}$ conferred a >500% fitness benefit over that of the wild-type enzyme at 32 μM MCN (Fig. 2 and Table 1). However, the enzymatic profiles of TetX2$_{S326I}$ and TetX2$_{F235Y}$ were very similar to those of the wild-type enzyme, showing no significant changes in the $K_{m(MCN)}$ and k_{cat} and only a slight increase in the $K_{m(NADPH)}$, suggesting that steady-state enzymatic parameters alone could not account for their observed beneficial effects on growth rates.

Small Changes of in Vivo Steady-State Protein Levels Also Prove to be Important for Increased Fitness. Fitness of cells with newly acquired mutations in an evolving population depends not only on the

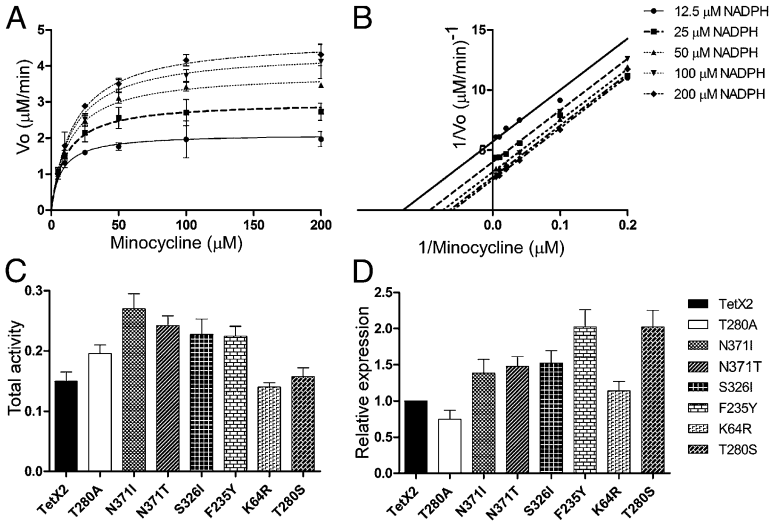

Fig. 3. The enzymatic performance of potential adaptive mutants from in vitro kinetics is well correlated with observed in vivo growth rates. Very small changes in $K_{m(MCN)}$ for TetX2$_{T280A}$ and TetX2$_{N371I}$ in the range of MCN concentrations used during experimental evolution provide a successful strategy for resistance. (*A*) Hydroxylation of MCN by TetX2 variants was monitored at 12.5, 25, 50, 100, and 200 μM of NADPH at 37 °C for 5 min (TetX2$_{T280A}$ shown here). The initial velocities were fit to the Michaelis–Menten ping-pong mechanism equation (Eq. **S1**). Error bars correspond to the standard -deviation among three individual measurements. (*B*) The double-reciprocal plot of MCN hydroxylation at various NADPH concentrations exhibits characteristics of binary complex formation. Error bars correspond to the SD among three individual measurements. Alternatively, TetX2$_{F235Y}$ and TetX2$_{T280S}$ appear at higher in vivo steady-state concentrations but are not able to have as much success within bacterial populations undergoing selection. (*C*) Activities of TetX2 and adaptive mutants were determined from cell lysates of chromosomally expressed enzymes in *E. coli* BW25113 at 50 μM MCN and 200 μM NADPH. Error bars correspond to standard deviation among six independent measurements. (*D*) Relative protein concentrations were determined by fitting initial velocities to Eq. **S1** and implementing kinetic parameters calculated in the in vitro kinetics assay. All data were normalized to the wild-type enzyme. Statistically significant differences in expression levels were observed for all mutants, compared with the wild type [using a pairwise *t*-test and sequential Bonferroni correction (27)], and were most noticeable for TetX2$_{F235Y}$ and TetX2$_{T280S}$. Error bars correspond to standard deviation among six independent measurements.

catalytic performance of a particular enzyme but also on its in vivo expression levels. Therefore, we quantified the expression levels of TetX2 mutants to test whether any of the variants might be present at higher steady-state concentrations in vivo. To test this hypothesis, TetX2 activity at three concentrations of MCN was measured from cell extracts of *E. coli* expressing chromosomally integrated *tet(X2)* variants (Fig. 3*C*). On the basis of the activities obtained from cell lysates, the relative enzyme concentrations of each mutant compared with those of the wild-type TetX2 were determined. As shown in Fig. 3*D*, the steady-state protein levels of $TetX2_{F235Y}$ and $TetX2_{T280S}$ are approximately twofold higher than those of the wild type; also $TetX2_{N371I}$, $TetX2_{N371T}$, and $TetX2_{S326I}$ appear at ~50% higher levels. The differences in the steady-state protein levels among the mutants are consistent with the growth rate data, which suggested that strains expressing $TetX2_{S326I}$ and $TetX2_{F235Y}$ were better at hydrolyzing MCN than wild-type TetX2. The in vitro kinetics together with the increased steady-state protein levels of these two mutants are consistent with the success of strains carrying $tet(X2)_{S326I}$, $tet(X2)_{T280S}$, and $tet(X2)_{F235Y}$.

Adaptive TetX2 Mutants Identified and Characterized in Vitro Provide the Basis for Quantitative ex Vivo Modeling of Fitness and Evolutionary Dynamics. The in vitro kinetic properties of the TetX2 variants were used to construct a mathematical model to quantitatively describe the growth rates of each adaptive mutation over a range of MCN concentrations (Fig. 4). Inhibition of bacterial growth rates by cytosolic MCN was determined by fitting the growth rate dependence of *E. coli* to MCN to a Hill function: $1-\frac{MCN^B}{A+[MCN]^B}$ (Eq. **S2**). At steady state, degradation of MCN by TetX2 equals the rate of diffusion of minocycline into the cell. The bisubstrate kinetics formulation (Eq. **S1**) and Fick's law were used to calculate the steady-state cytosolic MCN concentration from the total concentration of MCN (Eq. **S4**). The function determined by the inhibition of MCN on growth rates of *E. coli* was transformed onto the growth rates of the TetX2 variants, using the steady-state equation (Fig. 4*A*), and fitted using the measured values of $K_{m(MCN)}$, $K_{m(NADPH)}$, and k_{cat}. At higher concentrations of MCN, inhibition of cell growth is a consequence of the limited ability of TetX2 or a particular variant to inactivate MCN to tolerable levels.

Growth rates for *E. coli* carrying $tet(X2)_{T280A}$, $tet(X2)_{N371I}$, $tet(X2)_{N371T}$, and $tet(X2)_{K64R}$ could be predicted readily, considering largely kinetic parameters, whereas growth rates of $tet(X2)_{F235Y}$, $tet(X2)_{S326I}$, and $tet(X2)_{T280S}$ could be predicted reasonably only if their steady-state protein concentration was greater than that of the wild-type TetX2 (Fig. 4). This prediction was born out by in vivo activity measurements from cell extracts shown in Fig. 3*C*. As expected from the range of selection for MCN and bisubstrate kinetics, the fit for growth rates of *E. coli* with *tet(X2)* is most sensitive to K_m for MCN and is not as sensitive to K_m for NADPH under these selection conditions (*SI Materials and Methods*). The combination of $K_{m(MCN)}$ and k_{cat} determines the shape of the growth rate curves with the initial plateaus being particularly sensitive to $K_{m(MCN)}$. The measured k_{cat} values were similar for seven of the eight variants and therefore played a lesser role. The total activity affects the slope of the curve defining how severe the drop-off in growth rate responds to increasing MCN. The model cannot discriminate between changes in k_{cat} or changes in active protein concentration because these two variables affect the shape of the growth curve in the same way. The model underscores the strong correlation between the MCN concentration at which the most successful adaptive mutants, $tet(X2)_{T280A}$ and $tet(X2)_{N371I}$, were observed by experimental evolution (20–32 μM MCN) and their K_m to MCN (Table S3).

DNA Barcoding to Quantify the Allelic Frequency of the Seven Most Successful in Vitro *tet(X2)* Mutants. On the basis of growth rate and biochemical assays, we would expect both T280A and N371I to evolve. To test the success of mutants in evolving populations, we evolved 10 replicate populations of $BW25113_{tet(X2)}$ and tracked the rise and fall of the seven mutant alleles over the course of

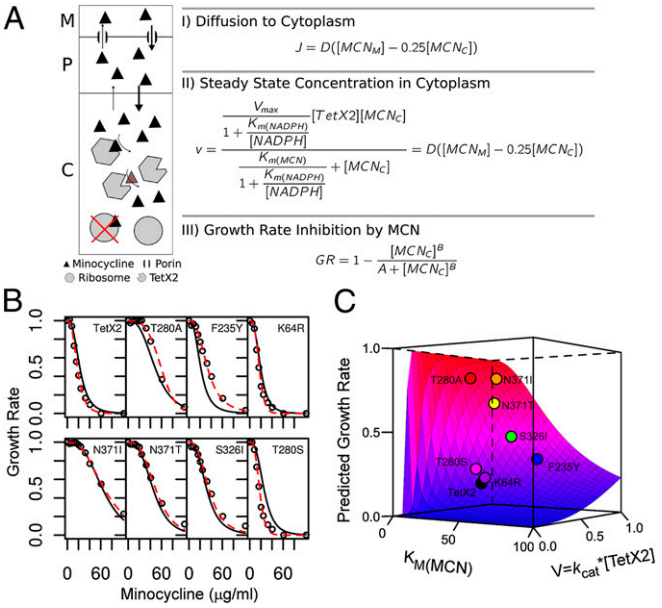

Fig. 4. Model incorporating in vitro enzyme kinetics and expression accurately predicts growth rates and can be used to construct the physicochemical fitness landscape of TetX2. (*A*) A mathematical model was built to predict the effect of TetX2 on reducing the inhibition of growth rates by MCN (*SI Materials and Methods*). (*B*) By transforming Eq. **S2** with Eq. **S4** we were able to accurately fit the measured growth rate, using in vitro kinetic parameters and estimates of protein concentration (solid line). The resulting model could then be used to predict $K_{m(MCN)}$ and total enzyme activity for each of the mutants from the measured growth rates (dashed line) for each mutant individually (Fig. S3 and Tables S3 and S4). (*C*) The physicochemical fitness landscape shows how changes in $K_{m(MCN)}$ and enzyme activity can affect growth rates at 32 μM MCN. Predicted growth rates from measured kinetic parameters for TetX2 (black), $TetX2_{T280A}$ (red), $TetX2_{N371I}$ (orange), $TetX2_{N371T}$ (yellow), $TetX2_{S326I}$ (green), $TetX2_{F235Y}$ (blue), $TetX2_{K64R}$ (purple), and $TetX2_{T280S}$ (magenta) are highlighted on the surface of the fitness landscape.

3 days undergoing selection at clinically relevant MCN concentrations. Adaptive mutations to *tet(X2)* can be identified from 10 to 32 μg/mL MCN (days 1–3) during a serial transfer experiment. Using the Illumina HiSeq sequencing system and a family of DNA barcodes, we were able to track changes in allelic frequencies for each of the characterized *tet(X2)* mutation sites at a resolution sufficient to identify a frequency of 0.5% with each population (*SI Materials and Methods*) (16). On average, each SNP was covered by 2.4×10^5 [95% confidence interval (CI): 3.7×10^4] reads (per population per day). As expected, $tet(X2)_{T280A}$ and $tet(X2)_{N371I}$ had the most success and appeared in 5 and 2 populations, respectively, whereas $tet(X2)_{K64R}$, $tet(X2)_{S326I}$, $tet(X2)_{N371T}$, and $tet(X2)_{F235Y}$ were not observed. Unexpectedly, $tet(X2)_{T280S}$ was observed in two populations despite data showing that the growth rates of $tet(X2)_{T280S}$ were equal to those of *tet(X2)*.

Crystal Structure of the Most Successful Adaptive TetX2 Mutant $TetX2_{T280A}$ Suggests an Indirect Effect on Protein Dynamics to Increase Enzyme Activity to MCN. To understand the role of the mutations in the mechanism of MCN hydroxylation, we determined the crystal structure of the most successful and kinetically efficient variant, $TetX2_{T280A}$, in complex with MCN at 2.7 Å resolution (Fig. 5 and Table S2). TetX2 is a monomer consisting of two domains, a larger N-terminal domain harboring a Rossmann fold responsible for interactions with the adenosine monophosphate of FAD and a smaller C-terminal domain that surrounds the catalytic cavity of the enzyme. The overall structure of $TetX2_{T280A}$ is very similar to that of the wild-type TetX2 [rmsd = 0.34 Å; Protein Data Bank (PDB) ID 3P9U] and 7-iodtetracycline(7-ITc):TetX2 complex structures (rmsd = 0.24 Å; PDB ID 2Y6Q) (17). MCN was found

in a similar conformation in the active site to 7-ITc with the hydrophilic portion of the substrate oriented toward the isoalloxazine ring of FAD (17). The structure clearly shows that position 280 is not directly involved in the catalytic mechanism of the enzyme and suggests that TetX2$_{T280A}$ alters kinetics indirectly perhaps through altered protein dynamics (*SI Materials and Methods* and Fig. S4).

Mapping of the other adaptive TetX2 mutations onto the crystal structure of the TetX2$_{T280A}$:MCN complex (Fig. 5) showed that all of the mutated residues, except TetX2$_{K64R}$ and TetX2$_{S326I}$, are located on the second domain of the protein, which is implicated largely in substrate recognition. Only residues at positions 235 and 371 are within 5 Å of MCN (Fig. 5*A*). The side chain of Phe235 is oriented 180° away from the substrate and makes van der Waal contacts within a hydrophobic pocket (Fig. 5*C*) but the polar hydroxyl group of Tyr235 in TetX2$_{F235Y}$ could readily satisfy a new hydrogen bond to Thr281, potentially stabilizing the protein. In contrast to position 235, the side chain of Asn371 is oriented directly toward the D-ring of MCN (~4.7 Å) (Fig. 5*A*) at the putative entrance site for tetracyclines. Substitution of a nonpolar residue (Ile) or a shorter polar side chain (Thr) at position 371 near the apolar pocket (Fig. 5*B*) results in smaller $K_{m(MCN)}$ and modest increases in k_{cat}. These findings clearly demonstrate that even mutations outside of the active site can have large effects on the fitness of the organisms.

Discussion

The molecular pathways accessible in protein evolution are defined by the mutation supply and the fitness effects of these mutations in the selective environment. In this study, we tested the hypothesis that on the basis of in vitro physicochemical properties of potential TetX2 adaptive mutants we could build a mathematical model that accurately predicts changes to fitness from biochemical first principles. In practice, this model is entirely reversible and permits the evaluation of specific changes to kinetic performance such as K_m, enzyme expression, and V_{max} from the growth rates of cells measured at varying substrate concentrations. Development of an accurate model relating growth rates to enzyme performance would also allow quantitative high-throughput screening of large libraries of enzyme variants without the need for arduous protein purification, facilitating investigation of enzyme adaptation in a highly systematic fashion (Fig. S4 and Table S3).

We chose the tetracycline-resistant enzyme, TetX2, as a model system to study the biophysical basis for adaptation to antibiotics. We identified a family of TetX2 variants and showed that growth rates of *E. coli* expressing chromosomal copies of the *tet(X2)* mutant alleles were exquisitely sensitive to MCN concentration and were tightly correlated to catalytic performance and steady-state expression levels of the TetX2 variants. On the basis of these experimental results, we were able to construct a mathematical model that consolidated the classic Michaelis–Menten kinetics and the relative in vivo expression levels to accurately and quantitatively predict growth rates and population dynamics.

Our work shows that small changes in kinetic parameters and steady-state protein concentrations can have large consequences on organismal fitness and adds to the repertoire of mechanisms through which drug resistance evolves. The success of TetX2 mutants with small improvements in catalytic performance over the wild-type TetX2 was reflected by large fitness benefits conferred by these variants in vivo as shown by growth rate assays (Table 1 and Fig. 2). We observed that the three mutants with the fastest growth rates at intermediate drug concentrations, TetX2$_{T280A}$, TetX2$_{N371I}$, and TetX2$_{N371T}$ produced at most a twofold decrease in $K_{m(MCN)}$ and, at most, a slight increase in k_{cat}. Even though the K_m for NADPH varied more widely among these three mutants, the in vivo concentration of NADPH is 5–10 times higher than that of MCN, making TetX2 performance less dependent on the concentration of NADPH under these selection conditions (18). A similar trend was observed for the mutant TetX2$_{K64R}$, which had growth rates and kinetics comparable to those of wild-type TetX2. The in vivo performance of TetX2$_{F235Y}$ and TetX2$_{T280S}$ was linked to at most twofold changes in steady-state protein levels, again emphasizing the relevance of small changes in activity over the relevant range of selection to fitness. These combined effects on fitness are readily evident when overall activity is plotted as a function of $K_{m(MCN)}$ and k_{cat}[TetX2] to build a physicochemical fitness landscape for TetX2 (Fig. 4*B*).

Why might small steps in enzyme performance be more common during selection? First, mutations that result in only modest changes to enzyme performance are more common than those with large changes (19, 20). As shown by our results, even very modest changes in physicochemical performance can have very strong fitness effects, depending on the context of selection. As long as a mutation alters protein performance sufficiently to meet the physiological needs of the cell, there is no necessary advantage to an enzyme that is "better" in terms of in vitro performance than others (21, 22). In addition, as beneficial mutations accumulate there is a general trend toward negative epistasis that shapes the adaptive landscape (1, 23).

Second, mutational spectra can change with the inherent DNA replication, recombination, and repair efficiencies of an organism as well as with the manner in which selection conditions induce stress (24, 25). Whereas we often envision selection as a harsh filter on populations, niche invasion can be a more gradual series of events wherein cells can work at the periphery of a condition, using the smaller, more numerous, and therefore more accessible ensemble of molecular trajectories afforded by protein structure and function. Although there has been much interest in changes to enzyme function that dramatically alter kinetic parameters, it is more likely that much more modest changes in enzyme performance may represent the more common adaptive pathway.

Our work shows that on the basis of molecular properties of the adaptive mutants of TetX2, we can accurately predict the success of mutant alleles during adaptation to antibiotic. As shown in Fig. S5, serial passages of 10 populations showed that in vitro enzyme kinetics correctly predicted the most successful adaptive alleles *tet(X2)*$_{T280A}$ and *tet(X2)*$_{N371I}$. Of the 7 populations where adaptive mutations to *tet(X2)* were observed, 5 contained *tet(X2)*$_{T280A}$ and *tet(X2)*$_{N371I}$ whereas 2 showed the presence of an allele that would be close to neutral, *tet(X2)*$_{T280S}$. The remaining four *tet(X2)* alleles

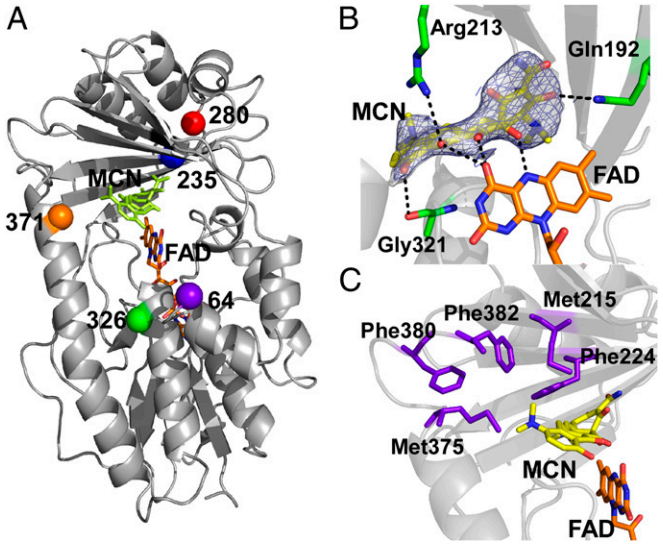

Fig. 5. Structure of the most efficient variant, TetX2$_{T280A}$, in complex with MCN at 2.7 Å resolution. (*A*) Ribbon representation of TetX2$_{T280A}$ structure with MCN shown in yellow and FAD in orange as sticks. The position of each adaptive point mutation is indicated as a sphere: 280 (red), 371 (orange), 326 (green), 235 (blue), and 64 (purple). (*B*) Active site of TetX2$_{T280A}$ illustrating residues interacting with MCN with 2Fo-Fc SIGMAA-weighted electron density map contoured at 1σ. (*C*) View of the active site with conserved nonpolar residues shown in purple.

predicted to have little or no success according to the in vitro data did not appear at our level of detection (≥0.5% of the overall population). Although it is possible that $tet(X2)_{T280S}$ may have an as yet unidentified fitness benefit, this was not observed in growth rate of the chromosomally expressed gene, enzyme kinetics of the purified enzyme, MIC determination from the chromosomal clone, or assays of crude extracts. The unexpected success of $tet(X2)_{T280S}$ is a cautionary tale and may support an important role for mutation supply, clonal interference, and epistasis in evolutionary dynamics (6, 7). Taken together, these studies show that physicochemical and structural properties of enzymes can be used to construct a quantitative prediction of fitness that can be used in conjunction with experimental evolution to explore the role of even the most modest changes in physical properties to large consequences to organismal fitness during natural selection.

Materials and Methods

Library Construction. *Tet(X2)* mutants were made using error-prone PCR following the manufacturer's protocols (GeneMorphII Random Mutagenesis Kit; Agilent Technologies). An appropriate *tet(X2)* library with one to two mutations per reaction was generated and subcloned into pUC19 (Invitrogen) to generate *tet(X2)*/pUC19 vector (*SI Materials and Methods*). *Tet(X2)* mutants that conferred the same or higher MIC relative to wild-type *tet(X2)* were isolated by plating at 4 μg/mL of MCN. DNA sequencing of 35 colonies identified seven *tet(X2)* mutants: $tet(X2)_{T280A}$, $tet(X2)_{N371I}$, $tet(X2)_{N371T}$, $tet(X2)_{F235Y}$, $tet(X2)_{S326I}$, $tet(X2)_{T280S}$, and $tet(X2)_{K64R}$.

Construction of Recombinant Strains. Integration of *tet(X2)* or variants into the chromosome of *E. coli* strain BW25113 was performed using a short homology recombineering approach (12). Briefly, *tet(X2)* was amplified from *tet(X2)*/pUC19 and used as a template for recombination into the *spc* operon of *E. coli* between *prlA* (SecY) and *rmpJ* (L36) to generate $BW25113_{tet(X2)}$ (*SI Materials and Methods*).

Growth Assays. Growth assays were performed in a 96-well plate format, using the Synergy 2 Multi-Mode Microplate Reader (BioTek Instruments). Single colonies of *E. coli* carrying different *tet(X2)* variants were used to inoculate overnight cultures and subsequently diluted to a final OD_{600} of 0.01. Growth at OD_{600} was monitored in 5-min intervals over 24 h at MCN concentrations ranging from 0 to 50 μg/mL. The fastest growth was defined as a slope of a tangent parallel to linear log-phase growth (*SI Materials and Methods* and Fig. S2).

Protein Expression and Purification. All proteins were overexpressed in *E. coli* BL21(DE3) Star (Agilent Technologies) with cleavable N-terminal 6×His_{tag} and purified as described previously (*SI Materials and Methods*) (26).

Kinetic Studies. Steady-state kinetic parameters were measured using a previously described, but modified TetX2 activity assay (14) (*SI Materials and Methods*). Steady-state kinetic parameters were determined by fitting initial reaction rates (υ_0) to a ping-pong mechanism (Eq. S1).

TetX2 Activity from Cell Extracts. In vivo TetX2-mediated inactivation of MCN was estimated from cell extracts prepared from each of the *E. coli* BW25113 cell lines expressing chromosomal copies of wild-type and mutant *tet(X2)*. Background levels of MCN inactivation activity were determined from extracts of BW25113 without *tet(X2)*. Cells were grown in lysogeny broth (LB) without MCN at 37 °C and harvested by centrifugation at an OD ∼ 0.6–0.8 before lysis by sonication. The steady-state TetX2 activity for inactivation of MCN by the soluble crude extracts was assayed using the previously described in vitro assay. TetX2 activity was measured at 25, 50, and 200 μM MCN at 200 μM of NADPH. All measurements were done in triplicate. The total amount of protein in each cell lysate was estimated by Bradford assay to account for variability in the efficiency of cell lysis. Relative enzyme concentrations were calculated from Eq. S1, where $V_{max} = k_{cat}[E_0]$, and E_0 = total enzyme concentration.

Structure Determination and Refinement. Crystallization of $TetX2_{T280A}$ was performed under similar conditions to those of the wild-type TetX2 (26). The structure was solved by molecular replacement, using 3P9U as a search model (*SI Materials and Methods*). The structure coordinates and amplitudes were deposited as 3V3N.

Serial-Passage Evolution Experiment. The MIC of *E. coli* $BW25113_{tet(X2)}$ in liquid culture was determined to be 16 μg/mL MCN in LB at 37 °C. To determine when changes to *tet(X2)* could be observed, serial passage experiments were initiated at 10 μg/mL MCN and increased daily as 10, 16, 24, 36, 52, 80, 120, 180, 300, and 320 μg/mL MCN. DNA samples for deep sequencing of 10 independent replicates was obtained from populations at 10, 16, and 24 μg/mL MCN. Each day 50 μL of the population was transferred to a new condition and 1-mL samples were frozen at −80 °C for DNA sequencing and characterization.

DNA Barcoding. We received 81 barcode plasmids containing distinct barcode sequences as a gift from the Marx Laboratory at Harvard University (Cambridge, MA) (16) (*SI Materials and Methods*).

ACKNOWLEDGMENTS. The authors thank Jay Nix for collecting X-ray data at Advanced Light Source. We also thank Drs. John S. Olson and Matthew R. Bennett for their advice and Rolf Lohaus for help with the growth curve analyses. This work was supported by National Institutes of Health Grant R01AI080714 (to Y.S.). The Rice University Crystallographic Core Facility is supported by a Kresge Science Initiative grant.

1. Chou HH, Chiu HC, Delaney NF, Segre D, Marx CJ (2011) Diminishing returns epistasis among beneficial mutations decelerates adaptation. *Science* 332(6034):1190–1192.
2. Khan AI, Dinh DM, Schneider D, Lenski RE, Cooper TF (2011) Negative epistasis between beneficial mutations in an evolving bacterial population. *Science* 332(6034):1193–1196.
3. Weinreich DM, Delaney NF, Depristo MA, Hartl DL (2006) Darwinian evolution can follow only very few mutational paths to fitter proteins. *Science* 312(5770):111–114.
4. Saxer G, Doebeli M, Travisano M (2010) The repeatability of adaptive radiation during long-term experimental evolution of Escherichia coli in a multiple nutrient environment. *PLoS ONE* 5(12):e14184.
5. Tenaillon O, et al. (2012) The molecular diversity of adaptive convergence. *Science* 335 (6067):457–461.
6. Arjan JA, et al. (1999) Diminishing returns from mutation supply rate in asexual populations. *Science* 283(5400):404–406.
7. Lang GI, Botstein D, Desai MM (2011) Genetic variation and the fate of beneficial mutations in asexual populations. *Genetics* 188(3):647–661.
8. Elena SF, Lenski RE (2003) Evolution experiments with microorganisms: The dynamics and genetic bases of adaptation. *Nat Rev Genet* 4(6):457–469.
9. Dean AM, Thornton JW (2007) Mechanistic approaches to the study of evolution: The functional synthesis. *Nat Rev Genet* 8(9):675–688.
10. Dykhuizen DE, Dean AM, Hartl DL (1987) Metabolic flux and fitness. *Genetics* 115(1):25–31.
11. Sniegowski PD, Gerrish PJ, Lenski RE (1997) Evolution of high mutation rates in experimental populations of E. coli. *Nature* 387(6634):703–705.
12. Datsenko KA, Wanner BL (2000) One-step inactivation of chromosomal genes in Escherichia coli K-12 using PCR products. *Proc Natl Acad Sci USA* 97(12):6640–6645.
13. Clinical and Laboratory Standards Institute (2006) *Quality Control Minimal Inhibitory Concentration (MIC) Limits for Broth Microdilution and MIC Interpretive Breakpoints* (Clinical and Laboratory Standards Institute, Wayne, PA).
14. Yang W, et al. (2004) TetX is a flavin-dependent monooxygenase conferring resistance to tetracycline antibiotics. *J Biol Chem* 279(50):52346–52352.
15. Cleland WW (1989) The kinetics of enzyme-catalyzed reactions with two or more substrates or products. I. Nomenclature and rate equations. 1963. *Biochim Biophys Acta* 1000:213–220.
16. Chubiz LM, Lee MC, Delaney NF, Marx CJ (2012) FREQ-Seq: A rapid, cost-effective, sequencing-based method to determine allele frequencies directly from mixed populations. *PLoS ONE* 7(10):e47959.
17. Volkers G, Palm GJ, Weiss MS, Wright GD, Hinrichs W (2011) Structural basis for a new tetracycline resistance mechanism relying on the TetX monooxygenase. *FEBS Lett* 585 (7):1061–1066.
18. Bennett BD, et al. (2009) Absolute metabolite concentrations and implied enzyme active site occupancy in Escherichia coli. *Nat Chem Biol* 5(8):593–599.
19. Romero PA, Arnold FH (2009) Exploring protein fitness landscapes by directed evolution. *Nat Rev Mol Cell Biol* 10(12):866–876.
20. Soskine M, Tawfik DS (2010) Mutational effects and the evolution of new protein functions. *Nat Rev Genet* 11(8):572–582.
21. Peña MI, Davlieva M, Bennett MR, Olson JS, Shamoo Y (2010) Evolutionary fates within a microbial population highlight an essential role for protein folding during natural selection. *Mol Syst Biol* 6:387.
22. Couñago R, Chen S, Shamoo Y (2006) In vivo molecular evolution reveals biophysical origins of organismal fitness. *Mol Cell* 22(4):441–449.
23. Garland T, Rose MR (2009) *Experimental Evolution: Concepts, Methods, and Applications of Selection Experiments* (Univ of California Press, London).
24. McKenzie GJ, Harris RS, Lee PL, Rosenberg SM (2000) The SOS response regulates adaptive mutation. *Proc Natl Acad Sci USA* 97(12):6646–6651.
25. Rosenberg SM, Hastings PJ (2003) Microbiology and evolution. Modulating mutation rates in the wild. *Science* 300(5624):1382–1383.
26. Walkiewicz K, Davlieva M, Wu G, Shamoo Y (2011) Crystal structure of Bacteroides thetaiotaomicron TetX2: A tetracycline degrading monooxygenase at 2.8 Å resolution. *Proteins* 79(7):2335–2340.
27. Rice WR (1989) Analyzing tables of statistical tests. *Evolution* 43:223–225.